High Aspect Ratio SiO₂ Capillary Based On Silicon Etching and Thermal Oxidation Process for Optical Modulator

N. V. Toan, S. Sangu, T. Saitoh, N. Inomata, T. Ono

Abstract—This paper presents the design and fabrication of an optical window for an optical modulator toward image sensing applications. An optical window consists of micrometer-order SiO_2 capillaries (porous solid) that can modulate transmission light intensity by moving the liquid in and out of porous solid. A high optical transmittance of the optical window can be achieved due to refractive index matching when the liquid is penetrated into the porous solid. Otherwise, its light transmittance is lower because of light reflection and scattering by air holes and capillary walls. Silicon capillaries fabricated by deep reactive ion etching (DRIE) process are completely oxidized to form the SiO_2 capillaries. Therefore, high aspect ratio SiO_2 capillaries can be achieved based on silicon capillaries formed by DRIE technique. Large compressive stress of the oxide causes bending of the capillary structure, which is reduced by optimizing the design of device structure. The large stress of the optical window can be released via thin supporting beams. A 7.2 mm x 9.6 mm optical window area toward a fully integrated with the image sensor format is successfully fabricated and its optical transmittance is evaluated with and without inserting liquids (ethanol and matching oil). The achieved modulation range is approximately 20% to 35% with and without liquid penetration in visible region (wavelength range from 450 nm to 650 nm).

Keywords—Thermal oxidation process, SiO_2 capillaries, optical window, light transmittance, image sensor, liquid penetration.

I. INTRODUCTION

ACQUIRING three-dimensional (depth) information by using a camera system has attracted attention in the field of image-sensing applications, such as object identification by in-vehicle camera [1] and machine vision applications [2]-[4]. The light field camera, where microlens array is employed [5], [6], is one of solutions to record such imagery information. The microlens array is located in front of an image sensor and serves as an output image pixel. A disadvantage of the usage of the microlens array is a trade-off relationship between the spatial and angular resolutions. A promising option to replace the microlens array is coded aperture imaging [7], [8], where refractive optical elements, such as lenses, are not used.

N.V. Toan is with Microsystem Integration Center (μSIC), Tohoku University, Sendai 980-8579, Japan (phone: +81-22-795-5806; e-mail: nvtoan@nme.mech.tohoku.ac.jp).
S. Sangu and T. Saitoh are with Core Technology Research & Development Center, Ricoh Institute of Technology, Natori City, 981-1241, Japan.
N. Inomata with Microsystem Integration Center (μSIC), Tohoku University, Sendai 980-8579, Japan.
T. Ono is with Graduate School of Engineering, Tohoku University, Sendai 980-8579, Japan.

Images from multiple apertures will overlap at the surface of the image sensor and then a computational algorithm is performed to reconstruct the original image. However, its disadvantage is low optical transmittance due to reflection and scattering effects caused by the air holes and inner walls pinholes, which results in a low signal-to-noise ratio. Therefore, devices capable of the integration of the image sensor for the high resolution light field information are still urgent requirements for functional image sensing applications.

For purpose of an optical modulator, porous solid was proposed in [9], where optical modulation can be achieved by moving a liquid in and out of the porous solid. In order to obtain high optical transmittance, SiO_2 is a suitable material as a modulator material. Also SiO_2 is widely used in micro devices because of its superior dielectric properties. SiO_2 films can be formed by a variety of methods including thermal oxidation, low pressure chemical vapor deposition (LPCVD), sputtering, etc. Unfortunately, deposited thick SiO_2 film generally has very high stress that causes cracking or peeling in the film [10], [11]. A low stress SiO_2 film can be deposited by plasma enhanced CVD (PECVD). SiO_2 can be patterned by reactive ion etching (RIE) method [12-13]. However, due to etching anisotropy and low selectivity against a mask material, the aspect ratio of fabricated structures is limited. A trench filling of low stress SiO_2 by using PECVD and sub-atmospheric chemical vapor deposition (SACVD) has been studied in [14]. However, the aspect ratio is not so high and the voids are easily formed during the filling process.

Dry etching technologies of silicon have been studied for many years, and have well developed recently. The etching process of silicon has easily done by deep RIE technique with high aspect ratio structure [12], [15], [16]. Silicon can be oxidized and converted to SiO_2 by employing thermal oxidation process as mentioned in [17], [18]. Nevertheless, formed SiO_2 layers have a high compressive stress due to volume expansion that causes bending or fracturing of device structures.

Basically, a high aspect ratio of SiO_2 capillaries using oxidation process can be achieved from the capillaries structure with thin silicon sidewalls by a combination of electron beam (EB) lithography [16], [19] or nano-imprint [20] techniques and deep RIE. In this research, fabrication process of high aspect ratio SiO_2 capillaries using a combination of deep RIE of Si and thermal oxidation technique is proposed. A repeating process of oxidation and etching is investigated and performed in order to obtain thin

silicon sidewalls of capillaries before final oxidation step. The large compressive stress of the oxide is reduced by optimizing the design of device structure. Moreover, an application of SiO_2 capillaries with and without liquid insertion has been proposed for obtaining high resolution light field information and their optical characteristics are evaluated. A FEM simulation using COMSOL software has been also performed in order to compare with experimental results.
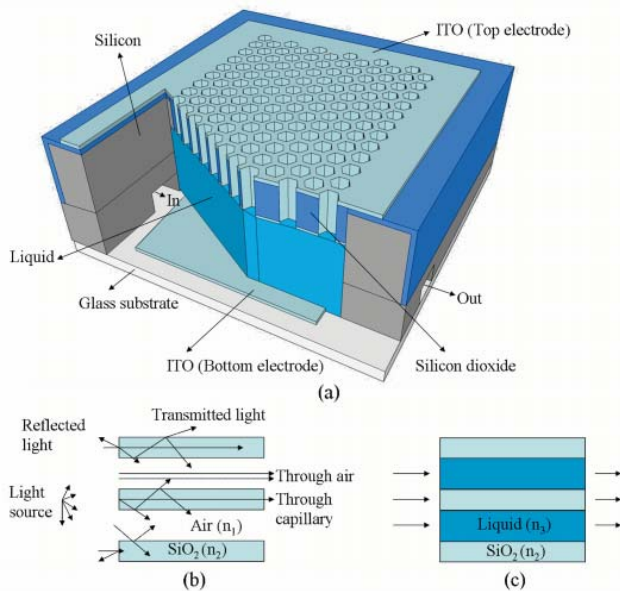
II. DEVICE STRUCTURE AND WORKING PRINCIPLE

Fig. 1 (a) Device concept, (b) Opaque state, (c) Transparent state

The device concept and working principle are elaborated as shown in Fig. 1. Its structure is basically consisted of micrometer-order SiO_2 capillaries (porous solid), a top indium tin oxide (ITO) electrode, a bottom ITO electrode, liquid and a glass substrate. The device can be directly mounted on an image sensor chip and is expected to have a large optical modulation range for functional image sensing applications.

The operation of this device is based on electro-wetting phenomenon-controlled capillary force [21]-[23]. When a DC voltage is applied to the structure, the liquid moves into the capillaries. Therefore, the porous solid gets transparent due to the refractive index matching. The reflected light inside of the capillaries will be disappeared because of refractive index matching at the interface ($n_2 = n_3$). Thus, a high optical transmittance will be obtained (Fig. 1 (c)). In case without liquid in the capillaries, the light transmittance of the capillary is lower than that with liquid because of the reflected light by air holes and capillary walls (Fig. 1 (b)) and it works ideally as an opaque state. Thus, by shifting the liquid in and out of the porous solid, the light transmittance can be electrically controlled.

III. FABRICATION PROCESS DESCRIPTION AND EXPERIMENTAL RESULTS
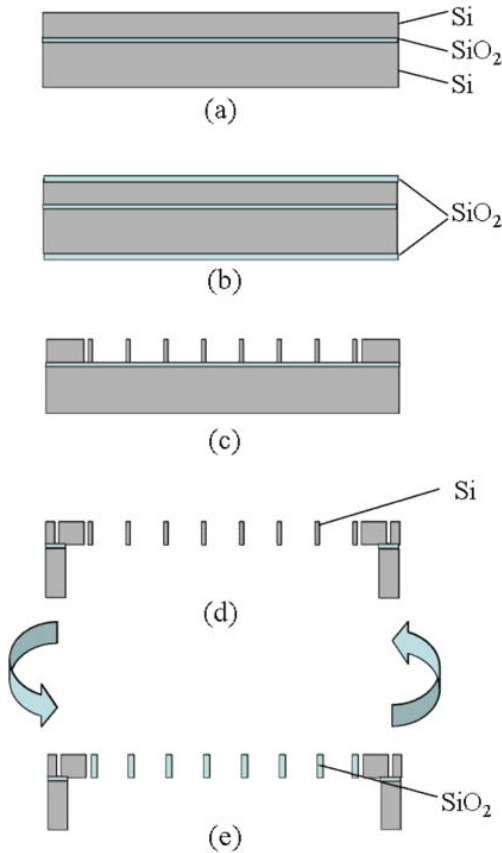

Fig. 2 Fabrication process: (a) SOI wafer (b) Thermal oxidation (c) Photolithography, RIE and deep RIE (d) Backside photolithography, deep RIE and SiO_2 removal (e) Repeating oxidation process

The fabrication process of the capillary plate is illustrated in Fig. 2. The fabrication process begins with a silicon on insulator (SOI) wafer, which consists of a 7 μm-thick top silicon device layer, 1 μm-thick oxide layer and 300 μm-thick silicon handling layer (Fig. 2 (a)). A 400 nm-thick SiO_2 layer is formed on the SOI wafer by wet thermal oxidation as an etching mask of the silicon device layer (Fig. 2 (b)). On this SiO_2 layer, a resist pattern is formed by immersion photolithography. Then, the SiO_2 layer is etched by using reactive ion etching (RIE) using a gas mixture of CHF_3 and Ar with a power of 120 W and a chamber pressure of 5 Pa. The micro-capillary structures are formed by using DRIE by Bosch process using SF_6 and C_4F_8 for short etching and passivation cycles (etching time 2.5 s, passivation time 2.5 s) for creating low scallops (Fig. 2 (c)). Next, the backside photolithography and deep RIE are performed, and then SiO_2 of the box layer is etched in HF solution for releasing the optical window structures, as the fabrication result of the 7.2 mm x 9.6 mm optical window is shown in Fig. 3 (a). A thin silicon sidewall of around 600 nm and silicon capillaries of around 1.3 μm diameter are achieved as shown in Fig. 3 (b).
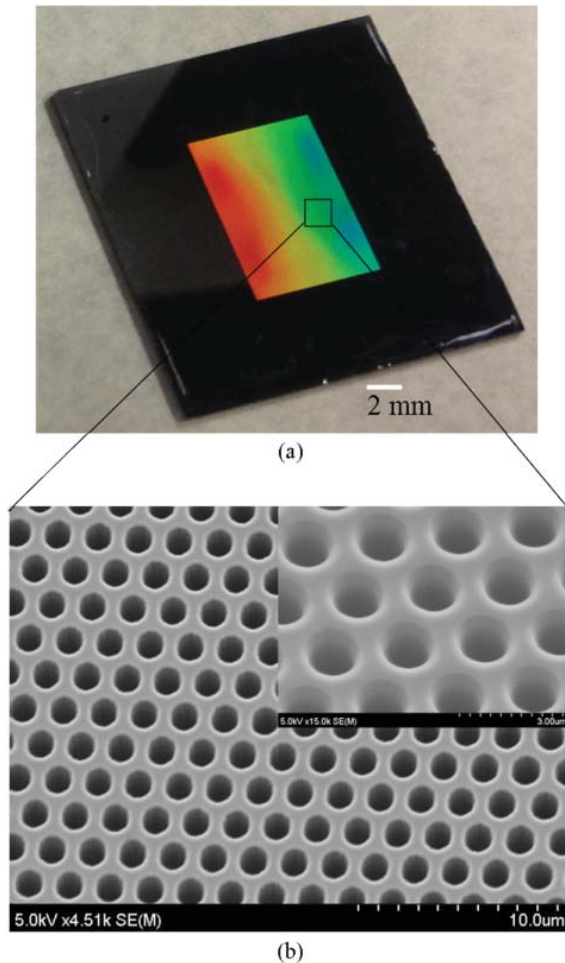
Fig. 3 (a) Silicon optical window (b) Close-up view of silicon capillaries

Fig. 4 (a) Silicon capillaries after repeating oxidation process (b) SiO$_2$ capillaries after final oxidation process

The silicon capillaries are thermally oxidized to form SiO$_2$ capillaries (Fig. 2 (e)). However, approximately 44% of silicon at surface is consumed during the thermal oxidation process [17], [18]. Therefore, the repeating oxidation and etching processes are performed to achieve the thin silicon sidewalls of the capillaries as shown in Fig. 4 (a). The silicon sidewall width and capillary diameter have been reached to 150 nm and 1.75 μm, respectively, after three repeating times of wet thermal oxidation process under conditions of temperature at 1100 ^{o}C, O$_2$ flow rate of 0.5 l/min and oxidation time of 30 minutes. 600 nm-wide sidewall capillaries are finally obtained after the oxidation process as shown in Fig. 4 (b).

Thus, the silicon capillaries are completely converted into SiO$_2$ capillaries with dimensions of 7 μm depth, 600 nm sidewall width, and 1.3 μm capillary diameter. A high aspect ratio of SiO$_2$ capillaries with an aspect ratio of approximately 11.5 has been achieved. In order to obtain higher aspect ratio of SiO$_2$ capillary sidewalls, the thinner and deeper silicon capillary sidewalls are needed.
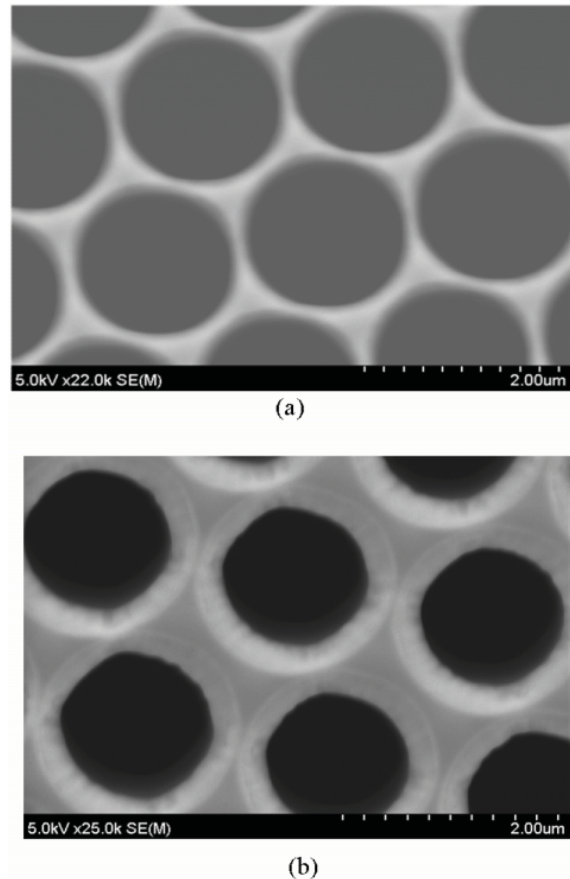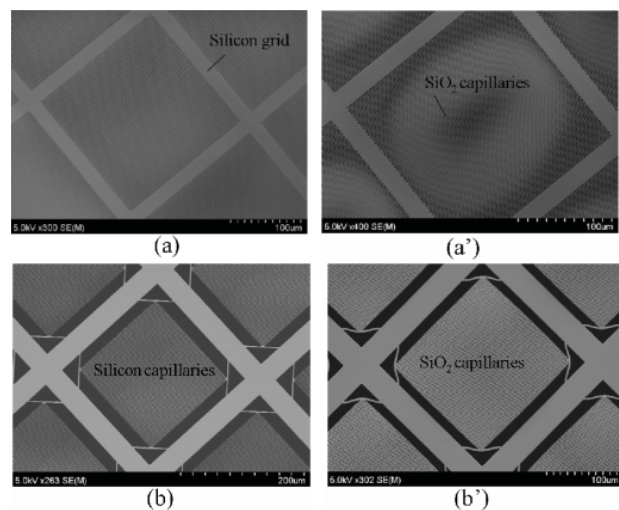

Fig. 5 SEM images of the optical windows (a) Before oxidation process of design #1 (a') After oxidation process of design #1 (b) Before oxidation process of design #2 (b') After oxidation process of design #2

Single crystalline silicon has no stress; therefore, no deformation is observed in the fabricated silicon optical

windows as shown in design #1 (Figs. 5 (a)) and design #2 (Figs. 5 (b)). When the silicon capillaries are turned into SiO_2 capillaries by using oxidation process, a large deformation is observed as shown in Figs. 5 (a'). This reason is due to compressive stress caused by the volume expansion of the structure during the oxidation process. In the design #1, the SiO_2 capillaries are supported by rigid silicon grid. The stress along horizontal direction cannot be released due to the silicon grid, as shown in Fig. 5 (a'). Therefore, the deformation is observed in the center of the optical window with approximately 10 μm of displacement in this design. In order to release the stress of the optical window structure, four thin beams at the corners with width of 1.5 um in the design #2 are employed, as shown in Figs. 5 (b) and (b'). The optical window does not bend after final oxidation step and the four thin supporting beams are bent by around 3 μm. It means that the stress into in-plane direction is reduced.

A FEM simulation of the relationship between displacement and stress is investigated, as shown in Fig. 6. The simulating parameters of design #1 and supporting beam of design #2 present in Table I. In the design #1, the highest deformation is located in the center of optical window (Fig. 6 (a)) and the stress is at center of the window edge (Fig. 6 (a')). When the optical window gets 10 um of displacement, it generates a high stress of 1900 MPa. A supporting beam is simulated only in the design #2. The correlative deformation of 3 um displacement (Fig. 6 (b)) of the beam structure has a high stress of 1870 MPa (Fig. 6 (b')). Thus, the high stress of the optical window (design #1) can be almost released via the thin supporting beams.

TABLE I
A RELATIONSHIP BETWEEN DISPLACEMENT AND STRESS OF DESIGN #1 AND SUPPORTING BEAM OF DESIGN #2

Dimensions	Design #1	Supporting beam of design #2
. Width (μm)	200	1.5
. Length (μm)	200	45
. Thickness (μm)	7	7
Total displacement (μm)	10	3
Stress (MPa)	1900	1870

IV. MEASUREMENT SETUP
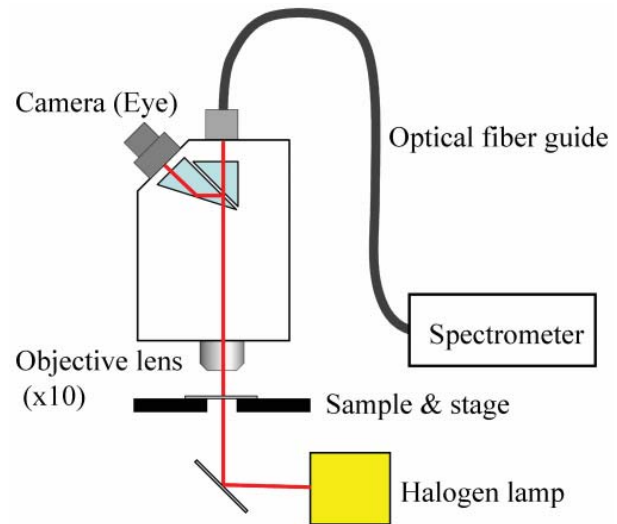
Fig. 7 Measurement setup

The optical measurement setup, sketched in Fig. 7, is used to evaluate the optical window characteristics. As shown in this figure, an optical microscope equipped with a spectrometer is employed for spectrum measurement in visible range and a halogen lamp is used for illumination via an aperture with a diameter of 10 mm. The distance between the source and the surface sample is around 300 mm.

V. MEASUREMENT RESULTS

A liquid (ethanol or matching oil) is inserted into the capillaries by just putting the liquid droplet on the device partly. A qualitative comparison of transmittances of the optical window structure, supported by four thin beams at corner, with and without liquid penetration is shown in Fig. 8 (a). Area of matching oil penetration becomes obviously clear than that without matching oil penetration through the captured image of Fig. 8 (a).

A quantitative comparison of transmittances with and without liquid penetration is shown in Fig. 8 (b) and Table II. A low transmittance of the optical window has been observed when it is measured in air environment without liquid penetration. The low transmission light in this case is due to the reflected light on the SiO_2 surfaces of the capillaries as explained before. Around 3% higher light transmission has been obtained with ethanol penetration (refractive index of ethanol: 1.36) than that with air environment (refractive index
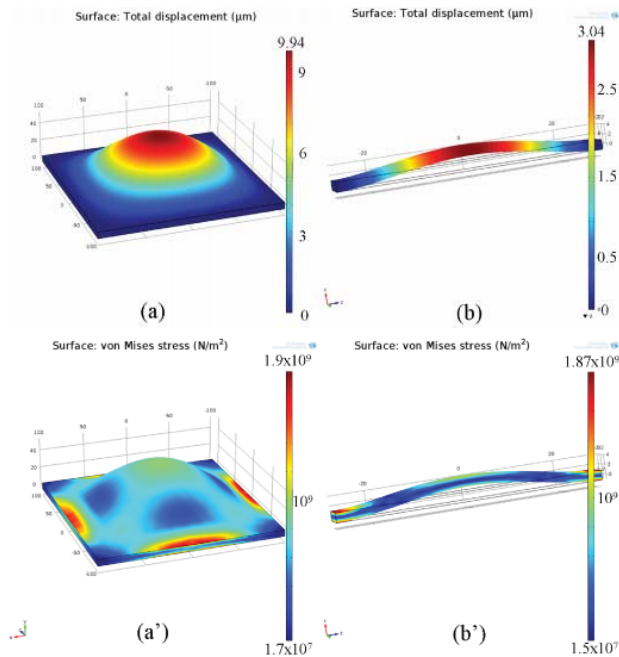

Fig. 6 FEM simulation (a) Displacement of design #1 (a') Stress of design #1 (b) Displacement of supporting beam of design #2 (b') Stress of supporting beam of design #2

of ethanol: 1). A higher transmitting light of around 20% to 35% can be achieved by using matching oil (refractive index of matching oil: 1.46) in a visible region from 450 nm to 650 nm. The possible reason is due to the refractive index matching with SiO_2 capillaries (refractive index of SiO_2: 1.45 to 1.49). Furthermore, a FEM simulation using COSOL software based on electromagnetic wave propagating has been performed, which is coincident with the measurement results.
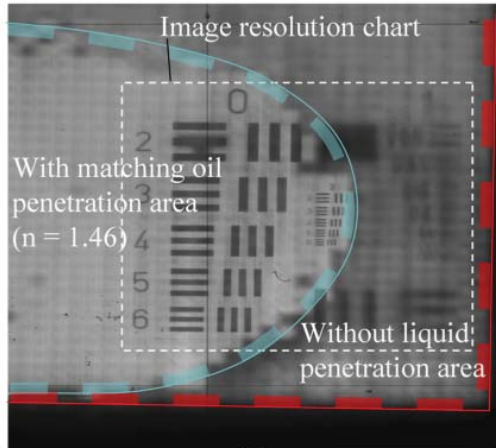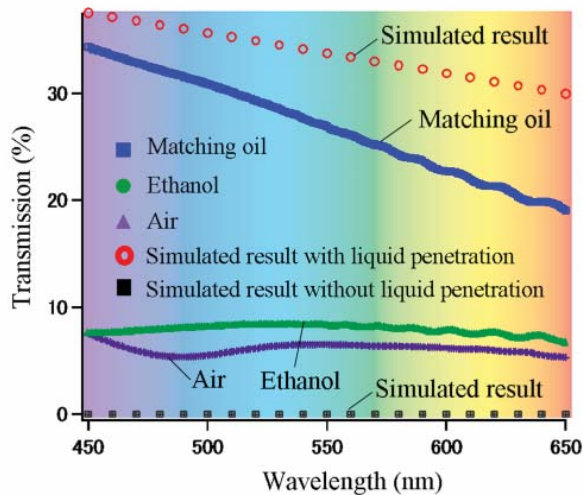
Fig. 8 (a) Optical image of test pattern via the optical window with and without liquid penetration areas (b) Evaluation of optical properties with and without inserting liquid

Silicon grids, existed in the current design (Fig. 5) may be absorbed light source; therefore, the light transmittance in case of liquid penetration is not so high (around 30%). A evaluation of the optical window which consists only of silicon grid (without SiO_2 capillary structure) show 36 % transmission (Table II). It means 64% of light transmission is reflected and absorbed by these silicon grid structures. It is necessary to remove them for higher optical modulation range in the further investigation. A FEM simulation indicates that 88% light transmittance can be obtained for the case without the silicon grid (Table II).

VI. CONCLUSIONS

In this paper, we have designed and fabricated optical windows consisted of micrometer-order SiO_2 capillaries for application of optical modulators. Additional evaluation of its optical characteristic has been also performed. A high aspect ratio of SiO_2 capillaries of around 11.5 has been achieved by employing thermal oxidation process. A very high compressive stress of oxidation process due to volume expansion is reduced by optimizing the design model. The high stress of optical window can be released via thin supporting beams. Its optical transmittance is evaluated under the conditions with and without liquid penetrations. The modulation range is approximately 20% to 35% for cases with and without matching oil in a wavelength range of visible region.

TABLE II
MEASUREMENT AND SIMULATION RESULTS AT WAVELENGTH OF 500 NM

State of optical windows	Transmission (%)
Air	5%
Ethanol	8%
Matching oil	31%
Simulated result without liquid penetration	0%
Simulated result with liquid penetration	35%
Optical window without capillaries	36 %
Simulated result with liquid penetration and without silicon grids	88%

REFERENCES

[1] G.D. Antoio, L.P. Jose, N. Manuel, P. Antonio, R. Santiago and O. Luis, "Locating moving object in car-driving sequences", *J. Image and video processing*, 24, pp. 1-23, 2014.
[2] H. Karaoguz, O. Erkent and H. I. Bozma, "RGB-D based place representation in topological maps", *J. Machine Vision and applications*, 25, pp. 1913-1927, 2014.
[3] J. Han, D. Wang, L. Shao, X. Qian, G. Cheng and J. Han, "Image visual attention computation and application via the learning of object atributes", *J. Machine Vision and applications*, 25, pp. 1671-1683, 2014.
[4] F. Liang, S.Tang, Y. Zhang, Z. Xu and J. Li, "Pedestrian detection based on sparse coding and transfer learning", *J. Machine Vision and applications*, 25, pp. 1697-1709, 2014.
[5] Ng. Ren, L. Marc, B. Mathieu, D. Gene, H. Mark, H. Pat, D. Duval, "Light field photography with a hand held plenoptic camera", Stanford *Tech Report CTSR* 2005-2.
[6] Ph. Nussbaum, R. Volkel, M. Eisner and S. Haselbeck, " Design, fabrication and testing of microlens arrays for sensors and microsystems", *Pure and applied optics: Journal of the European optical society part A*, 6, pp. 617-636, 1997.
[7] A. Levin, R. Fergus, F. Durand, B. Freeman, "Image and Depth from a Conventional Camera with a Coded Aperture", *in Proceedings of SIGGRAPH*, 2009.
[8] J. Heikenfeld, K. Zhou, E. Kreit, B. Raji, S. Yang, B. Sun, A. Milarcik, L. Clapp and R. Schwartz, "Electrofluidic displays using Young-Laplace

transposition of brilliant pigment dispersions" J. *Nature photon*, 3, pp. 292-296 2009.

[9] G. Beni and S. Hackwood, "Electro-wetting displays", *J. Appl. Phys. Lett.* 38, 207, 1981.

[10] A Szekeres and P Danesh, "Mechanical stress in SiO2/Si structures formed by thermal oxidation of amorphous and crystalline silicon", *Journal of Semicond. Sci. Technol*, 11, pp. 1225-1230, 1996.

[11] N.I. Morimoto, and J.W. Swart, "Development of a cluster tool and analysis of deposition of silicon oxide by TEOS O$_2$ PECVD", *MRS proceedings*, p. 263, 1996.

[12] N.V. Toan, T. Kubota, H. Sekhar, S. Samukawa and T. Ono, "Mechanical quality factor enhancement in a silicon micromechanical resonator by low-damage process using neutral beam etching technology", *J. Micromech. Microeng*, 24, 085005, 2014.

[13] H. Ohtake, H. Ishihara, T. Fuse, A. Koshiishi and S. Samukawa, "Highly selective and high rate SiO$_2$ etching using argon-added C$_2$F$_4$/CF$_3$I plasma", *Journal of vacuum science & technology B*, 21, p. 2142, 2003.

[14] C. Chang, T. Abe and M. Esashi, "Trench filling characteristics of low stress TEOS/ozone oxide deposited by PECVD and SACVD", *J. Microsystem Technologies*, 10, pp. 97-102, 2004.

[15] N.V. Toan, M. Toda, Y. Kawai and T. Ono, "A capacitive silicon resonator with a movable electrode structure for gap width reduction", *J. Micromech. Microeng*, 24, 025006, 2014.

[16] N.V. Toan, H. Miyashita, M. Toda, Y. Kawai and T. Ono, "Fabrication of an hermetically packaged silicon resonator on LTCC substrate", *J. Microsystem Technologies*, 19, pp. 1165-1175, 2013.

[17] D. Andriukaitis and R. Anilionis, "Oxidation process and different crystallographic plane orientation dependence simulation in micro and nano strucutre", *In proceedings of conf. on information technology and interfaces*, pp. 573-578, 2007.

[18] Y. Suzuki, K. Totsu, M. Moriyama, M. Esashi and S. Tanaka, "Free-standing subwavelength grid infrared rejection filter of 90 mm diameter for EUV light source", *In proceedings of the 27th IEEE international conference on micro electro mechanical systems*, pp. 482-485, 2014.

[19] C. Con, J. Zhang and B. Cui, "Nanofabrication of high aspect ratio structures using an evaporated reisist containing metal", *J. Nanotechnology*, 25, p. 17531, 2014.

[20] S.Y. Chou, P.R. Krauss and P.J. Renstrom, "Imprint lithography with 25-nanometer resolution", *Science*, 272, pp. 85-87, 1996.

[21] J. Heikenfeld, K. Zhou, E. Kreit, B. Raji, S. Yang, B. Sun, A. Milarcik, L. Clapp and R. Schwartz, "Electrofluidic displays using Young-Laplace transposition of brilliant pigment dispersions" J. *Nature photon*, 3, pp. 292-296 2009.

[22] B. Berge and J. Peseux, "Variable focal lens controlled by an external voltage: an application of electrowetting", *Eur. Phys. J. E*, 3, pp. 159-163, 2000.

[23] J. Lee, H. Moon, J. Fowler, T. Schoellhammer, and C.J. Kim, "Electrowetting and electrowetting on dielectric for micrscale liquid handling", *J. Sensor Actuator A*, **95**, pp. 259-268, 2002.

N.V. Toan received the B.S in 2006 and M.S. degree in 2009 in physics and electronics from University of Science, Vietnam National University, Ho Chi Minh City, Viet Nam. He received his Dr. Eng. degree with the research of silicon capable of integration of LSI for application of timing device from Tohoku University in 2014. He is working as a post doctorial researcher at Microsystem Intergration Center, Tohoku University. His current research interest is optical window with liquid penetration for application of optical modulator.

S. Sangu received the Dr. Eng. degree in electronics and information engineering from Hokkaido University in 1999. During 1999–2003, he has been a Researcher of the "Localized Photon" project for the Exploratory Research for Advance Technology (ERATO) at the Japan Science and Technology Corporation, Tokyo, Japan. Since 2003, he joined Ricoh Co. Ltd. as a Researcher. His current research interests are micro/nanophotonics and its application to optical devices. He is a member of the Japan Society of Applied Physics (JSAP).

T. Saitoh graduated from the School of Engineering, Tohoku University. During 1982–1986, he joined Toshiba Corp. as an Engineer of semiconductor single crystal growth technology. Since 1986 he joined Ricoh Co. Ltd. as an Engineer. His current research interests are MEMS/optical device and its application to optical systems.

N. Inomata received the B.S., the M.S., and the Dr.Eng. degrees from Tohoku University, Sendai, Japan, in 2008, 2010, and 2013, respectively. Since 2013, he has been an Assistant professor at Microsystem Integration Center, Tohoku University. His research areas are mainly applications of micro/nano electro mechanical systems, especially sensing systems using MEMS/NEMS.

T. Ono received the Dr. Eng. degree from Tohoku University in 1996. During 1996–2001, he has been a Research Associate in Graduate School of Engineering, Tohoku University. During 2001-2009, he has been an Associate Professor. He is currently a Professor in the department of Mechanical Systems and Design, Graduate School of Engineering at Tohoku University. Also He is a professor of Department of Mechanical Engineering, Graduate School of Engineering, The University of Tokyo. His research covers wide area including Microelectromechanical Systems (MEMSs), Nanoelectromechanical Systems (NEMSs), silicon based nanofabrication, ultrasensitive sensing based on resonating device, MEMS-LSI integration, optical modulators and scanning probe technologies. He is a member of the Japan Society of Applied Physics (JSAP) and The Japan Society of Mechanical Engineering (JSME), etc.